^{1}H NMR Study of the Heme Molecular Structure in Sperm Whale Met-Aquo and Met-Imidazole Myoglobins

Yasuhiko Yamamoto

Department of Chemistry, University of Tsukuba, Tsukuba 305

(Received May 13, 1996)

The resolved heme peripheral side-chain proton resonances of sperm whale met-aquo myoglobin have been connected to the corresponding resonances in met-imidazole myoglobin by the magnetization transfer through the external ligand exchange. From the signal assignments in met-imidazole myoglobin, which have been independently obtained using conventional two-dimensional NMR and one-dimensional nuclear Overhauser effect difference spectroscopies, the observed connectivities unambiguously identified the corresponding resonances of met-aquo myoglobin. The calculation of the pseudo-contact shifts for the resonances of met-aquo myoglobin from the reported zero-field splitting constant [Y. -H. Kao, and J. T. J. Lecomte, *J. Am. Chem. Soc.*, **115**, 9754—9762 (1993) and *J. Am. Chem. Soc.*, **116**, 6991 (1994)] together with the diamagnetic shifts observed for carbonmonoxy myoglobin [B. C. Mabbutt, and P. E. Wright, *Biochim. Biophys. Acta*, **832**, 175—185 (1985)], allowed the extraction of the contact shifts from their paramagnetic shifts. The heme peripheral propionate conformation in met-aquo myoglobin has been determined from the analysis of the contact shifts for the $C_\alpha H_2$ proton resonances. The obtained conformations agreed well with those described by the X-ray study [T. Takano, *J. Mol. Biol.*, **110**, 537—568 (1977)]. The thermal spin equilibrium in met-imidazole myoglobin has been analyzed using the mean heme methyl proton shift as an indicator for the spin state of the protein. The equilibrium populations determined from the analysis of the NMR shift data did not agree with those determined from the magnetic susceptibility measurements [T. Iizuka, and M. Kotani, *Biochim. Biophys. Acta,* **181**, 275—286 (1969)], indicating that the heme methyl proton shifts cannot be used as quantitative probe for the thermal spin equilibrium in met-imidazole myoglobin. This would be attributed to the temperature-dependent delocalization of the unpaired electron density from the heme iron to the porphyrin π system and the axial ligands due to the perturbation on the coordination structure around the iron, exerted by the steric repulsion between the bound imidazole and the imidazole side-chain of the distal His residue, as revealed by the X-ray study [C. Lionetti, M. G. Guanziroli, F. Frigerio, P. Ascenzi, and M. Bolognesi, *J. Mol. Biol.*, **217**, 409—412 (1991)].

NMR is one of the most powerful spectroscopic techniques for investigating the detailed structure of hemoprotein in all oxidation and spin-states.[1,2] In the paramagnetic hemoprotein, the heme peripheral side-chain proton resonances are resolved outside the diamagnetic envelope, where signals due to the protein overlap severely, and provide particularly sensitive probes for the heme environments. Met-aquo myoglobin (metMb(H_2O)[#]) represents one of the two cases in paramagnetic hemoproteins, in which the observed paramagnetic shifts for the resonances arising from heme and amino acid residues in the active site can be quantitatively analyzed in terms of their electronic/molecular structure.[3,4] Only limited signal assignments, however, have been reported so far for metMb(H_2O).[4—7] This is mostly due to the fact that hyperfine shifted resonances in the spectrum of metMb(H_2O) exhibit extremely short relaxation times (a few ms) and therefore usual multi-pulse experiments for detecting the connectivities in dispensable for the signal assignments cannot be applied to this system.[8] Hence, although NOE connectivity has been observed between the selected hyperfine shifted proton resonances of the protein,[6,9] the signal assignments of the heme peripheral proton resonances in metMb(H_2O) have been heavily relied on the selective isotope labeling.[5,7]

In the present study, we focus on the signal assignments of the resolved heme peripheral side-chain proton resonances in metMb(H_2O), which corrected a tentative assignment[6] previously proposed. We have demonstrated that the magnetization transfer through the ligand exchange is particularly useful for assigning the hyperfine shifted resonances of paramagnetic hemoproteins, with their relaxation rates comparable to or preferably smaller than the ligand exchange rate in the system.[10—13] Our assignment is based on a two-step process. First, the signal assignments of met-imidazole Mb (metMb(Im)) are obtained from the dipolar and scalar connectivities observed by conventional 1D and 2D NMR techniques and second, the resonances for metMb(Im) and metMb(H_2O) are connected by the magnetization transfer through the external ligand exchange between H_2O and imidazole. The present assignment strategy can be also ap-

#*Abbreviations*: Mb, myoglobin, metMb(H_2O) or metMb(D_2O), met-aquo myoglobin; metMb(Im), met-imidazole myoglobin; NOE, nuclear Overhauser effect.

plied for the resonances arising from amino acid protons in metMb(H_2O). With the unambiguous signal assignments, the analysis of the hyperfine shifts yielded the heme peripheral side-chain conformations in metMb(H_2O). We discuss an approach for studying the molecular structure of the heme in metMb(H_2O), where the measurements of the NMR parameters useful for the analysis, such as spin-spin coupling[14] and the cross-relaxation rate,[15] are impractical due to the excessive paramagnetic relaxation.[16]

Additionally, the thermal spin equilibrium between high-spin, $S=5/2$, and low-spin, $S=1/2$, states in metMb complexed with the external ligand of the intermediate field strength, such as imidazole, N_3^- or OH^-, has been studied extensively by a variety of techniques including magnetic susceptibility measurement,[17—21] ESR,[22] IR,[23,24] Mössbauer,[25] optical,[26] and NMR[27—34] spectroscopies. In the NMR study of the thermal spin equilibrium in hemoprotein,[27—34] heme methyl proton resonances are most frequently used as probe signals for monitoring the spin state of the protein. The thermal spin equilibrium in metMb(Im) has been analyzed in detail from the temperature dependence of the heme methyl proton resonances.[27,28] The temperature dependence of individual heme methyl proton shift, however, reflects the hyperfine shift pattern of that resonance for a given position of the equilibrium. On the other hand, the mean of the four heme methyl proton shifts is expected to serve as a simple indicator for the spin state of the protein, because in-plane asymmetry of the heme electronic structure is likely to be compensated by averaging their shifts.[32—34] The unambiguous assignments of all the four heme methyl proton resonances in metMb(Im) allow the analysis of the thermal spin equilibrium in this Mb complex using the mean heme methyl proton shift. The equilibrium population determined from the analysis did not agree with that obtained from the magnetic susceptibility measurements.[19] This result indicates that the heme methyl proton shift cannot be used as a quantitative indicator for the thermal spin equilibrium in metMb(Im). This could be attributed to the temperature-dependent coordination structure around the heme iron in metMb(Im), exerted by the steric repulsion between the bound imidazole and the imidazole side-chain of distal His residue,[35] which largely influences the spin transfer pattern and concomitantly the heme methyl proton hyperfine shifts.

Experimental

Sample Preparation: Sperm whale Mb was purchased as a lyophilized powder from Biozyme and used without further purification. Imidazole was obtained from Sigma Chemical Co. Solutions for NMR measurements were 1.0×10^{-3} mol dm^{-3} in protein in D_2O. The pD of the samples was adjusted using NaOD or DCl and was measured using a Horiba F-22 pH meter equipped with a Horiba 6069-10C electrode.

NMR Measurements: ^{1}H NMR spectra were recorded using Bruker AC-400 FT-NMR spectrometer operating at a ^{1}H frequency of 400 MHz in the quadrature mode. A typical spectrum consisted of 2k transients with 16k data points over 100 kHz band width and a 5.3 μs 45° pulse. The residual water resonance was suppressed with a 0.1 s presaturation decoupler pulse. Saturation transfer experiments were carried out by selectively saturating a desired peak for 50 ms. The spectra resulted from the saturation transfer experiments were presented in the form of difference spectra. NOE difference spectra of metMb(Im) were recorded by selectively saturating 2-vinyl α-proton or 1-Me resonance for 50 ms and the results were presented in the form of NOE difference spectra. Two-dimensional shift correlated spectroscopy (COSY) of metMb(Im) was recorded with the standard pulse sequence. The 512 free induction decays were acquired with 2k data points and a spectral width of 30 kHz. The time-domain data matrix was expanded to 1k×2k by zero-filling. A sine bell function was used to apodize the spectrum in both dimensions and the spectrum was presented in the absolute value mode. Chemical shifts are given in ppm downfield from sodium 2, 2-dimethyl-2-silapentane-5-sulfonate with the residual HDO as an internal reference.

Results

Imidazole Titration of MetMb(D_2O): The downfield hyperfine shifted portion of the 400 MHz ^{1}H NMR spectra of sperm whale metMb(D_2O) at pD 6.99 and 35 °C is illustrated in A of Fig. 1. Signals resolved at >30 ppm arise from the heme peripheral protons and have been assigned by selective deuteration and NOE connectivities.[5,6] With the addition of imidazole as an external ligand, the intensity of the signals at 10—40 ppm for metMb(Im) increase at the expense of those for metMb(D_2O). The difference in total spin between metMb(D_2O) ($S=5/2$)[19] and metMb(Im) (mainly $S=1/2$)[19] results in a large separation of resonances arising from both forms, which permits independent observation of their signals. The difference in the resonance frequency of>10 kHz between the corresponding heme methyl proton signals for the two forms indicates that the ligand exchange rate is $<10^3$ s^{-1}. This results are consistent with the kinetic data for imidazole binding to metMb(H_2O), i.e., $k_{on}=170$ dm^3 mol^{-1} s^{-1} and $k_{off}=5.4$ s^{-1} at 25 °C in 0.1 mol dm^{-1} of KNO_3.[36]

Signal Assignments: The saturation transfer difference spectra recorded on the mixture of metMb(D_2O) and metMb(Im) ([metMb(D_2O)]/[metMb(Im)]=2.5) at pD 6.99 and 50 °C are illustrated in Fig. 2. Saturation of a selected resonance for metMb(D_2O) exhibits a clear saturation transfer to the corresponding resonance for metMb(Im). With the known signal assignments for the resolved heme peripheral side-chain proton resonances of metMb(D_2O), the corresponding resonance for metMb(Im) can be identified through the connectivities shown in the figure. Simultaneously, the assignment for metMb(D_2O) can also be confirmed from the signal assignments for metMb(Im), which were independently obtained from the observation of dipolar and scalar connectivities. Two single-proton resonances at 31.65 and 42.56 ppm, which have been unambiguously attributed to the vinyl α-protons using the Mb reconstituted with [2,4-($C_\alpha D)_2$] hemin,[5] have been tentatively assigned to 2- and 4-vinyl α-protons, respectively.[6] The signal at 42.56 ppm exhibits the saturation transfer connectivity to the peak at 22.70 ppm of metMb(Im), as illustrated in Fig. 2. The vinyl β-protons associated with the α-proton resonating at 22.70 ppm can be clearly identified from the characteristic COSY cross

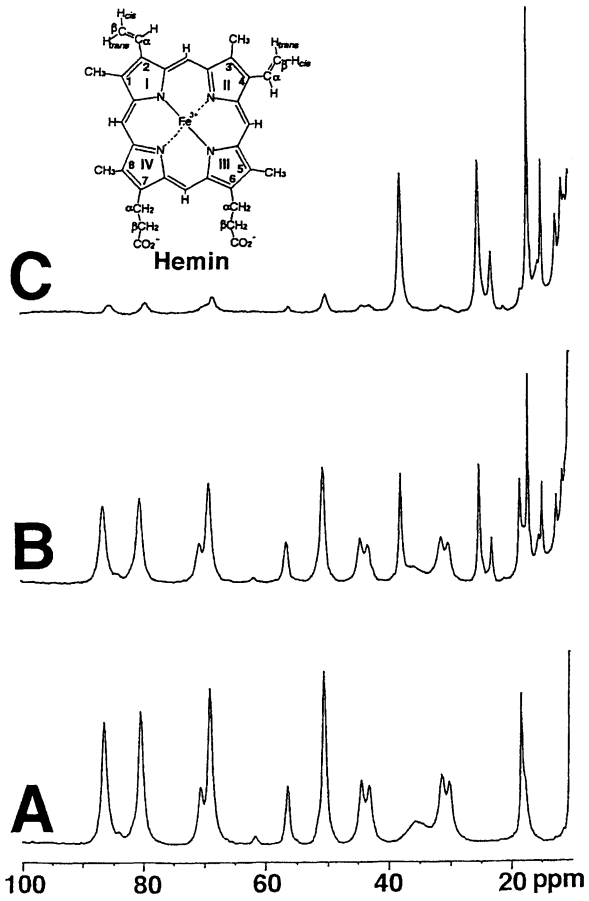

Fig. 1. Downfield hyperfine shifted portions of the 400 MHz ^{1}H NMR spectra of 1.0×10^{-3} mol dm^{-3} sperm whale metMb(D_2O) at pD 6.99 and 35 °C (A) and in the presence of 3×10^{-4} mol dm^{-3} of imidazole (B) and 0.01 mol dm^{-3} of imidazole (C). The signals arising from metMb(Im) are observed at < 40 ppm and, with the addition of imidazole, the intensity of these signals increases at the expense of those for metMb(D_2O). Molecular structure and numbering system of hemin is illustrated in the inset.

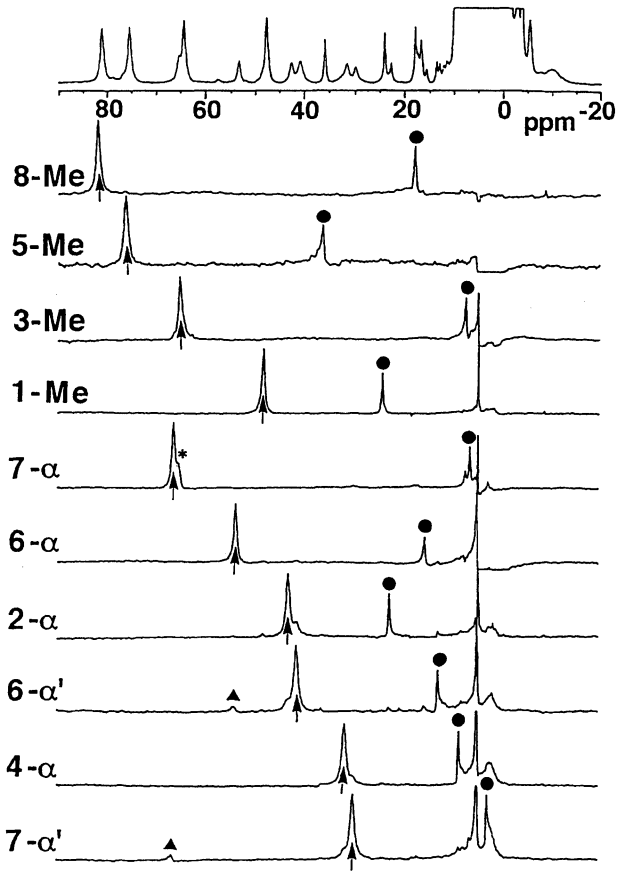

Fig. 2. The 400 MHz ^{1}H NMR spectrum and saturation transfer difference spectra of the mixture of metMb(D_2O) and metMb(Im) at pD 6.99 and 50 °C. [metMb(D_2O)/metMb(Im)] = 2.5. The signal assignments are indicated with the spectra. The arrows indicate the peaks saturated and the peaks exhibiting the magnetization transfer through the ligand exchange are indicated by filled circles. The * sign shows the signal due to off-resonance saturation. The peaks indicated by filled triangles are due to NOE.

peaks[37] at −0.47 and −1.43 ppm, shown in B of Fig. 3. 1D NOE difference spectra resulted from the saturation of this vinyl α-proton and 1-Me resonances for 50 ms are illustrated in traces C and D of Fig. 3. Saturation of the vinyl α-proton peak at 22.70 ppm exhibits NOEs to the two vinyl β-proton resonances and the difference in the magnitude between the observed NOEs for the peaks at −0.47 and −1.43 ppm dictates their assignments to β_{cis} and β_{trans} protons, respectively. Saturation of 1-Me resonance exhibits a relatively large NOE to the β_{trans} proton, as shown in the trace D. These results indicate both that these protons belong to the heme 2-vinyl group and that the orientation of this vinyl group with respect to the porphyrin in metMb(Im) is in *cis*-conformer. Hence the saturation transfer connectivities shown in Fig. 2 indicate that the peak at 42.56 ppm arises from 2-α proton of metMb(D_2O) and the other vinyl α-proton signal at 31.65 ppm is attributable to 4-α. Moreover, the estimated 2-vinyl conformation for metMb(Im), i.e. *cis*-conformer, is essentially consistent with that in the X-ray crystal structure.[35]

Temperature Dependence of Heme Methyl Proton Resonances for MetMb(Im): The heme methyl proton resonances, 1-, 5-, and 8-Me, of metMb(Im) are resolved outside of the diamagnetic envelope. The elusive 3-Me signal resonating in the diamagnetic region can be clearly identified through the saturation transfer connectivity shown in Fig. 2. The Curie plots, observed shift versus reciprocal of absolute temperature, for all heme methyl proton resonances, together with that for the mean of the four heme methyl proton shift, are illustrated in Fig. 4. The thermal spin equilibrium in metMb(Im) is clearly manifested in the anti-Curie behavior of the mean shift.

Discussion

Heme Molecular Structure in MetMb(D_2O): In paramagnetic compounds, the obtained shift (δ_{obsd}) arises from two contributions

$$\delta_{obsd} = \delta_{dia} + \delta_{para} \quad (1)$$

δ_{dia} is the diamagnetic term and δ_{para} is the paramagnetic

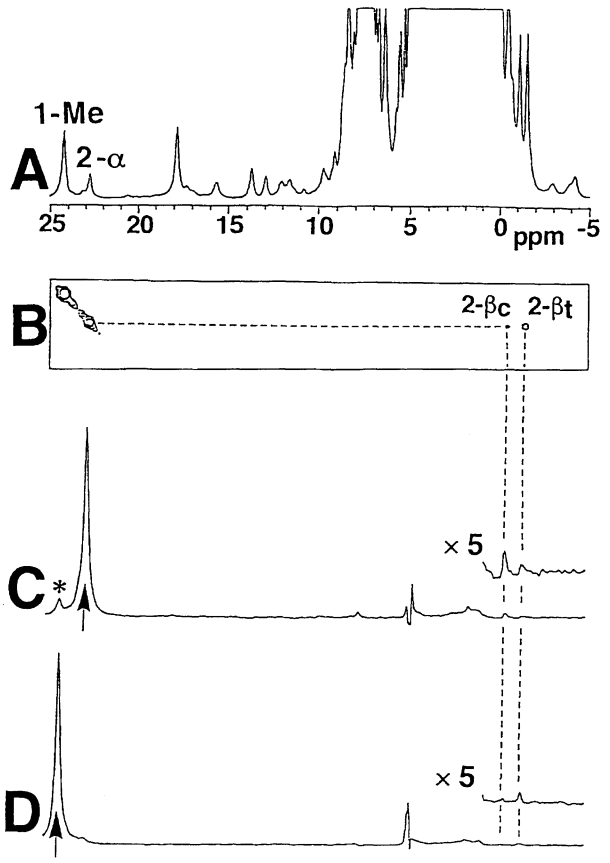

Fig. 3. 1D and 2D spectra recorded on metMb(Im) at pD 6.99 and 50 °C. A portion, −5—25 ppm, of the 400 MHz ^{1}H NMR spectrum (A). A portion of the COSY spectrum (B). 2-β_c and 2-β_t indicate 2-vinyl β_{cis} and β_{trans} protons, respectively. The 1D NOE difference spectrum with the saturation of 2-α proton resonance (C). 2-β_c proton resonance exhibits larger NOE than 2-β_t. The signal indicated by * is due to off-resonance saturation. The 1D NOE difference spectrum with the saturation of 1-Me proton resonance (D). 2-β_t proton resonance exhibits larger NOE than 2-β_c.

term which is due to unpaired electron effects. The shifts for carbonyl or oxo Mb are generally used as δ_{dia}. δ_{para} can be divided into two terms, i. e. contact (δ_c) and pseudo-contact (δ_{pc}) shifts. δ_c is observable for nuclei onto which the unpaired electrons are delocalized. δ_{pc} stems from the anisotropic magnetic moment. In the case of the $S=5/2$ system such as metMb(D_2O), δ_{pc} arises largely from sizable zero-field splitting.[4] δ_{pc} in metMb(H_2O) has been quantitatively determined[4] so that, provided that the spatial relationship between the nucleus and unpaired electron is known, δ_{pc} for a given nuclei can be calculated. The results from the analysis of the δ_{obsd} values for the selected resonances of metMb(D_2O) are summerized in Table 1.

δ_c is proportional to the hyperfine coupling constant, A_H, which is related to the spin density on the resonating nucleus. A_H for heme propionate α-proton is expressed as[38]

$$A_H = (1/2S)Q_{CCH}\rho_c \quad (2)$$

where S is the total spin, Q_{CCH} is the parameter that accounts

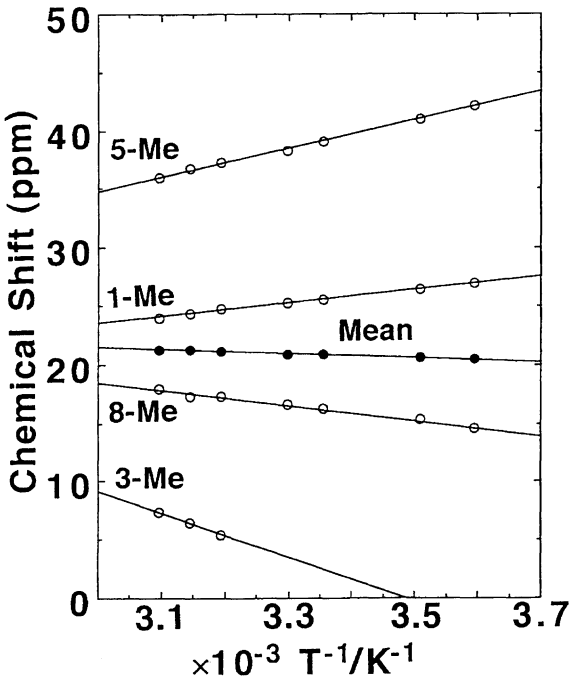

Fig. 4. Curie plot, the observed shift versus reciprocal of absolute temperature, for heme methyl proton resonances (open circles) and the mean heme methyl proton shift (filled circles) of metMb(Im) in D_2O at pD 6.99. The 3-Me shift data above 3.3×10^{-3} K^{-1} were extrapolated using those below 3.2×10^{-3} K^{-1}.

Table 1. Chemical shift[a] of Selected Heme Peripheral Side-Chain Proton Resonances in MetMb(H_2O) and MetMb-(Im) at 50 °C

Assignment	δ_{obsd}	δ_{dia}[b]	δ_{para}	δ_{pc}[c]	δ_c	δ(Im)
1-Me	47.65	3.63	44.02	4.6	39.4	24.03
3-Me	64.38	3.79	60.59	4.6	56.0	7.32
5-Me	75.47	2.53	72.94	4.6	68.3	35.90
8-Me	81.05	3.59	77.46	4.6	72.9	17.86
2-α	42.56	8.43	34.13	4.6	29.0	22.70
4-α	31.65	8.62	23.03	3.7	19.3	8.48
6-α	53.36	4.21	49.15	3.5	45.7	15.62
6-α'	40.77	4.21	36.56	4.6	32.0	12.81
7-α	64.40	4.21	61.19	3.3	57.9	6.38
7-α'	29.88	4.21	25.67	4.0	21.7	2.69

a) Shifts in ppm. b) Diamagnetic shift obtained from published carbonyl myoglobin data.[54] c) Pseudo-contact shift calculated from the reported zero-field splitting[4] constant and then corrected to 50 °C using the T^{-2} dependency.

for the transfer of the unpaired electron density in the p_Z orbital of the pyrrole carbon to the proton of interest and ρ_c is the unpaired electron density. Q_{CCH} is not a constant, but is dependent on θ, the dihedral angle between the C–C_α–H plane and the normal to the heme plane, as defined in A of Fig. 5, according to[39]

$$Q_{CCH} = B_0 + B_2\cos^2\theta \quad (3)$$

where B_0 and B_2 are coefficients. Since B_0 is much smaller than B_2, the magnitude of their δ_c values,[40] to the first ap-

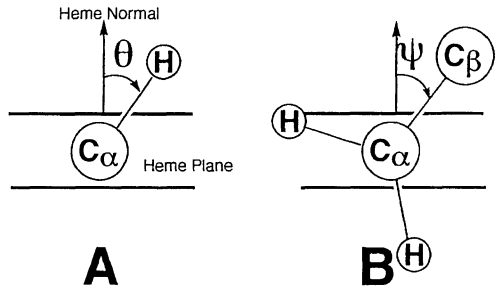

Fig. 5. (A) Dihedral angle θ is defined as the angle between the pyrrole C, Cα, H plane and the normal to the heme plane. (B) Dihedral angle ψ is defined as the angle between the pyrrole C, Cα, Cβ plane and the normal to the heme plane. The rotation direction for these dihedral angles is positive when the viewer is located on the Cα atom and observe a clockwise rotation around the bond.

proximation, is assumed to be proportional to $\cos^2\theta$.[41] Consequently, the ratio between the δ_c values for the propionate α-CH_2 geminal proton resonances is correlated to the propionate conformation and is plotted as a function of the dihedral angle, ψ, between the C–Cα–Cβ plane and the heme normal (see B of Fig. 5) in Fig. 6. Due to the symmetric nature of the CH_2 group, multiple conformational states are obtained from an given ratio, as illustrated in the plot. For the 6-propionate α-CH_2 group, the ratio (this ratio is calculated as the smallest δ_c divided by the largest δ_c for the α-CH_2 geminal protons and hence the ratio should be between 0 and 1.) of 0.70 yields the ψ values of $\pm9°$, $\pm87°$, $\pm93°$, and $\pm171°$. Similarly, the ratio of 0.37 yields the ψ values of $\pm23°$, $\pm82°$, $\pm98°$, or $\pm167°$, for the 7-propionate α-CH_2 group. Among the possible ψ, the values close to $\pm90°$, are not consistent with

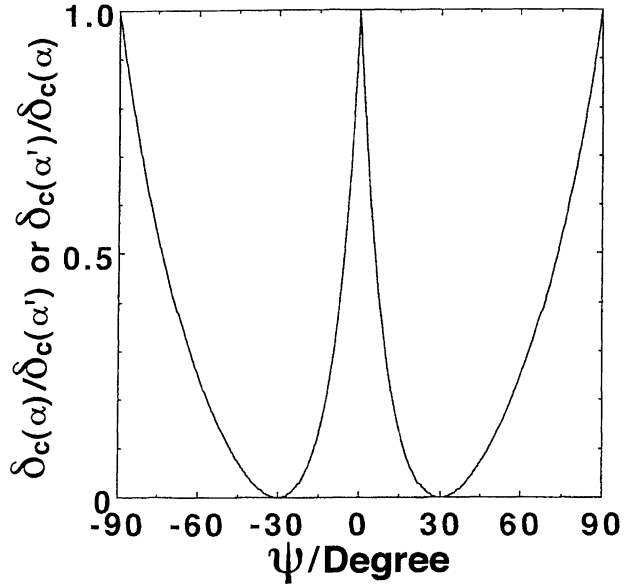

Fig. 6. Plot of the ratio between the heme propionate CαH_2 geminal proton contact shifts versus ψ. The plots for $-90° < \psi < 90°$ are shown. The ratio is calculated as the smallest δ_c divided by the largest δ_c for the geminal protons. ψ is defined in Fig. 5B.

the reported NOE connectivities between the propionate α-protons and nearby heme methyl proton in the present Mb, which indicated that one of the α-CH_2 proton is much closer to the nearby heme methyl proton than the other.[6] Hence, $\pm9°$, $\pm171°$ and $\pm23°$, $\pm167°$ can be selected as the candidates for the ψ values of the 6- and 7- propionate α-CH_2 groups, respectively. Consequently, although the ψ value cannot be determined uniquely from the present analysis, it is at least concluded that the C–Cα–Cβ plane of the heme propionate in metMb(D_2O) is nearly orthogonal to the heme plane. Such heme propionate conformations are similar to those determined in the single crystal, i.e. the ψ values have been shown to be $-173.5°$ and $-12.2°$ for the 6- and 7-propionate groups, respectively.[42] The conformation of the heme propionate group is fixed relative to not only the heme, but also to the protein by the salt-bridge between the carboxyl terminal of the group and amino acid side-chain, which is proposed to play an important role in correctly orienting the heme with respect respect to the protein.[43—48] The δ_c values for the heme vinyl CαH proton resonances are also similarly interpreted in terms of the vinyl conformation. However, in addition to the direct interaction of the 1s orbital of vinyl CαH proton with the porphyrin π system, which, as described above in the case of the heme propionate α-proton, is modulated by the dihedral angle θ, the unpaired electron density is also transferred to this proton from the vinyl Cα.[40] Although direct delocalization of the spin density within the extended π framework centered on carbon onto the proton is symmetry forbidden, sizable A_H has been reported in aromatic free radicals.[40] Furthermore, the unpaired electron density delocalized into the vinyl π system is crucially modulated through the vinyl conformation with respect to the porphyrin π system. δ_c of heme methyl proton signals are often used to assess the magnitude of the unpaired electron density residing in each pyrrole ring, because of the absence of θ dependency in their δ_c values.[49] Assuming that the δ_c values for 1- and 3-Me reflect the relative magnitude of the spin density in the pyrroles I and II (see the hemin structure in the inset of Fig. 1), the fact that the δ_c value for the latter is larger than that for the former is interpreted as the presence of larger spin density in pyrrole II than that in pyrrole I. In spite of such difference in the spin density between the pyrroles, 2-α proton attached to pyrrole I exhibits larger δ_c than 4-α proton of pyrrole II. Due to the difference in the mechanism of the spin delocalization, the two transfer processes operating on this proton, i.e. one is the delocalization of the spin through the direct interaction between the 1s orbital of this proton and the porphyrin π system (mechanism I) and the other is the transfer from the vinyl Cα (mechanism II), exhibit opposite signs in the hyperfine coupling constants (mechanism I and II induce downfield and upfield contact shifts, respectively.). The relative contributions from these spin transfer mechanisms to δ_c for the vinyl CαH proton are primarily determined by the vinyl conformation. For example, for the vinyl conformation with $\theta=\pm90°$, the contribution of mechanism II becomes significant because the π system of the porphyrin is efficiently extended to that of the

vinyl group, whereas mechanism I is minimum. Therefore the δ_c of vinyl $C_\alpha H$ proton could be negative. On the other hand, for the conformation with θ=0° or 180°, the maximum spin transfer via mechanism I results in large downfield shift for this proton resonance. Thus, the δ_c values for 2-α and 4-α protons dictate that the θ value for 4-α proton is closer to ±90° than that of 2-α. According to the X-ray structure of sperm whale metMb(H_2O),[42] both heme vinyl substituents are in *cis*-conformer with their π system close to the heme plane, i.e., θ was found to be about 60° for both the vinyl groups.[50] In contrast with the heme propionate conformation in the present Mb, the heme vinyl groups have been shown to possess considerable internal mobility.[51,52] Equilibrium conformation, as manifested in NMR chemical shifts, about possible structural fluctuations dose not necessarily coincide with the ground state of the molecular structure which is essentially described in the X-ray studies. The present study strongly suggests the presence of a sizable difference in θ between 2- and 4- vinyl groups in metMb(D_2O).

Thermal Spin Equilibrium in MetMb(Im): Under the fast exchange between pure low-spin and pure high-spin states in metMb(Im), δ_{obsd} is expressed as a weighed average:

$$\delta_{obsd} = \zeta\delta_{obsd(LS)} + (1 - \zeta)\delta_{obsd(HS)} \quad (4)$$

where $\delta_{obsd(LS)}$ and $\delta_{obsd(HS)}$ represent the observed shifts of the resonance for low-spin and high-spin states of metMb(Im), respectively, and ζ is the fraction of low-spin state. In general, the shifts for met-cyano Mb (metMb(CN^-)) and metMb(H_2O) are considered to represent those for pure low-spin and pure high-spin metMb complexes, respectively.[1,53] The mean shifts of the four heme methyl proton resonances for metMb(H_2O), metMb(CN^-), and metMb(Im) are summarized in Table 2. The substitution of the mean δ_{obsd} values for the three metMb complexes into Eq. 4 yielded the ζ values of 0.91 and 0.88 at 25.0 and 50.0 °C, respectively. These values are compared with those determined from the magnetic susceptibility measurements, i.e. 0.86 and 0.60 at 25.0 and 50.0 °C, respectively.[19] The ζ value tends to be overestimated in the analysis of the mean heme methyl proton hyperfine shifts and the difference became larger at higher temperature. Since the heme methyl proton shift essentially reflects the magnitude of the unpaired electron density which resides in the p_z orbital of the pyrrole carbon to which the methyl group is covalently bonded, any change in the spin transfer from the iron to the porphyrin π system induces sizable alteration in their hyperfine shifts. Therefore the comparison of the ζ values obtained from the two different methods strongly suggested that the spin transfer from the iron to the porphyrin and the axial ligands in metMb(Im) is influenced by temperature. In the presence of the temperature-dependent delocalization of the unpaired electron density, the heme methyl proton hyperfine shifts cannot be interpreted solely in terms of the thermal spin equilibrium in the protein. The X-ray study revealed a large steric repulsion between the bound-imidazole and the side-chain of His E7 in metMb(Im).[35] Such steric hindrance between the two imidazole groups at the distal heme cavity would be one of the major structural factors for changes in the electronic structure of the heme in metMb(Im). Careful scrutiny is needed to determine which structural alteration occurs at the active site of metMb(Im).

Table 2. The Analysis of the Thermal Spin Equilibrium in MetMb(Im) Based on the Mean of the Four Heme Methyl Proton Shifts

Temp[a)]	$\overline{\delta_{obsd(HS)}}$ [b)]	$\overline{\delta_{obsd(LS)}}$ [b)]	$\overline{\delta_{obsd(Im)}}$ [b)]	ζ_{NMR} [c)]	ζ_χ [b)]
25.0	75.0	15.7	20.8	0.91	0.86
50.0	67.1	15.2	21.3	0.88	0.60

a) in °C. b) The mean of the four heme methyl shifts in ppm. HS, LS, and Im represent metMb(D_2O), metMb(CN^-), and metMb(Im), respectively. c) Fraction of low-spin state in metMb(Im) calculated from Eq. 4 in the text. d) Fraction of low-spin state in metMb(Im) determined from magnetic susceptibility measurements.[19]

References

1) J. D. Satterlee, *Annu. Rep. NMR Spectrosc.*, **17**, 79 (1986).
2) J. D. Satterlee, *Met. Ions Biol. Syst.*, **21**, 121 (1986).
3) S. D. Emerson and G. N. La Mar, *Biochemistry*, **29**, 1556 (1990).
4) Y. -H. Kao and J. T. J. Lecomte, *J. Am. Chem. Soc.*, **115**, 9754 (1993); *J Am. Chem. Soc.*, **116**, 6991 (1994).
5) G. N. La Mar, D. L. Budd, K. M. Smith, and K. C. Langry, *J. Am. Chem. Soc.*, **102**, 1822 (1980).
6) S. W. Unger, J. T. J. Lecomte, and G. N. La Mar, *J. Magn. Reson.*, **64**, 521 (1985).
7) S. S. Sankar, G. N. La Mar, K. M. Smith, and E. M. Fujinari, *Biochim. Biophys. Acta*, **912**, 220 (1987).
8) G. N. La Mar and J. S. de Ropp, "Biological Magnetic Resonance," ed by L. J. Berliner and J. Reuben, Plenum Press, New York (1993), Vol. 12, p. 1.
9) Y. Yamamoto, Y. Inoue, R. Chujo, and T. Suzuki, *Eur. J. Biochem.*, **189**, 567 (1990).
10) Y. Yamamoto, R. Chujo, Y. Inoue, and T. Suzuki, *FEBS Lett.*, **310**, 71 (1992).
11) Y. Yamamoto, Y. Inoue, and T. Suzuki, *Magn. Reson. Chem.*, **31**, S8 (1993).
12) Y. Yamamoto, *Biochem. Biophys. Res. Commun.*, **196**, 348 (1993).
13) Y. Yamamoto, T. Suzuki, and H. Hori, *Biochim. Biophys. Acta*, **1203**, 267 (1993).
14) D. Morikis, R. Brüschweiler, and P. E. Wright, *J. Am. Chem. Soc.*, **115**, 6238 (1993).
15) Y. Yamamoto, *J. Chem. Soc., Dalton Trans.*, **1995**, 3281.
16) J. T. J. Lecomte, S. W. Unger, and G. N. La Mar, *J. Magn. Reson.*, **94**, 112 (1991).
17) J. Beetlestone and P. George, *Biochemistry*, **3**, 707 (1964).
18) T. Iizuka and M. Kotani, *Biochim. Biophys. Acta*, **167**, 257 (1969).
19) T. Iizuka and M. Kotani, *Biochim. Biophys. Acta*, **181**, 275 (1969).
20) T. Iizuka and M. Kotani, *Biochim. Biophys. Acta*, **194**, 351 (1969).
21) C. Messana, M. Cerdonio, P. Shenkin, R. W. Noble, G. F. Fermi, R. N. Perutz, and M. F. Perutz, *Biochemistry*, **17**, 3652

(1978).
22) D. M. Scholler and B. M. Hoffman, *J. Am. Chem. Soc.*, **101**, 1655 (1979).
23) S. McCoy and W. S. Caughey, *Biochemistry*, **9**, 2387 (1970).
24) J. D. Allben and L. Y. Fager, *Biochemistry*, **11**, 842 (1972).
25) M. R. C. Winter, C. E. Johnson, G. Lang, and R. J. P. Williams, *Biochim. Biophys. Acta*, **263**, 515 (1972).
26) S. Neya, S. Hada, and N. Funasaki, *Biochemistry*, **22**, 3686 (1983).
27) T. Iizuka and I. Morishima, *Biochim. Biophys. Acta*, **371**, 1 (1974).
28) I. Morishima and T. Iizuka, *J. Am. Chem. Soc.*, **96**, 5279 (1974).
29) I. Morishima, S. Neya, T. Inubushi, T. Yonezawa, and T. Iizuka, *Biochim. Biophys. Acta*, **534**, 307 (1978).
30) S. Neya and N. Funasaki, *Biochemistry*, **25**, 1221 (1986).
31) Y. Yamamoto and G. N. La Mar, *Biochim. Biophys. Acta*, **996**, 187 (1986).
32) Y. Yamamoto, R. Chujo, and T. Suzuki, *Eur. J. Biochem.*, **198**, 285 (1991).
33) Y. Yamamoto, T. Suzuki, and H. Hori, *Biochim. Biophys. Acta*, **1248**, 149 (1995).
34) J. -Z. Wu, G. N. La Mar, K. -B. Lee, F. A. Walker, M. L. Chiu, and S. G. Sligar, *Biochemistry*, **30**, 2156 (1991).
35) C. Lionetti, M. G. Guanziroli, F. Frigerio, P. Ascenzi, and M. Bolognesi, *J. Mol. Biol.*, **217**, 409 (1991).
36) E. Antonini and M. Brunori, "Hemoglobin and Myoglobin in Their Reactions with Ligands," North-Holland Publishing Company, Amsterdam (1971), p. 230.
37) Y. Yamamoto, A. Osawa, Y. Inoue, R. Chujo, and T. Suzuki, *FEBS Lett.*, **247**, 263 (1989).
38) H. M. McConnell, *J. Chem. Phys.*, **24**, 764 (1956); *Proc. Natl. Acad. Sci. U.S.A.*, **43**, 721 (1957).
39) C. Heller and H. M. McConnell, *J. Chem. Phys.*, **32**, 1575 (1960).
40) G. N. La Mar, "NMR of Paramagnetic Molecules," ed by G. N. La Mar, W. D. Horrocks, Jr., and R. H. Holms, Academic Press, New York (1973), pp. 85—126.
41) U. Pandey, G. N. La Mar, J. T. J. Lecomte, F. Ascoli, M. Brunori, K. M. Smith, R. K. Pandey, D. W. Parish, and V. Thanabal, *Biochemistry*, **25**, 5638 (1986).
42) T. Takano, *J. Mol. Biol.*, **110**, 537 (1977).
43) G. N. La Mar, S. D. Emerson, J. T. J. Lecomte, U. Pandey, K. M. Smith, G. W. Craig, and L. A. Kehres, *J. Am. Chem. Soc.*, **108**, 5568 (1986).
44) S. Neya and N. Funasaki, *J. Biol. Chem.*, **262** 6275 (1987).
45) S. Neya and N. Funasaki, *Biochim. Biophys. Acta*, **952**, 150 (1988).
46) G. N. La Mar, U. Pandey, J. B. Hauksson, R. K. Pandey, and K. M. Smith, *J. Am. Chem. Soc.*, **111**, 485 (1989).
47) J. B. Hauksson, G. N. La Mar, R. K. Pandey, I. N. Rezzano, and K. M. Smith, *J. Am. Chem. Soc.*, **112**, 6198 (1990).
48) G. N. La Mar, J. B. Hauksson, L. B. Dugad, P. A. Liddel, N. Venkataramana, and K. M. Smith, *J. Am. Chem. Soc.*, **113**, 1544 (1991).
49) G. N. La Mar, "Biological Applications of Magnetic Resonance," ed by R. G. Shulman, Academic Press, New York (1979), pp. 305—343.
50) L. S. Reid, A. R. Lim, and A. G. Mauk, *J. Am. Chem. Soc.*, **108**, 8197 (1986).
51) S. Ramaprasad, R. D. Johnson, and G. N. La Mar, *J. Am. Chem. Soc.*, **106**, 3632 (1984).
52) Y. Yamamoto, K. Iwafune, N. Nanai, R. Chujo, Y. Inoue, and T. Suzuki, *Biochim. Biophys. Acta*, **1120**, 173 (1992).
53) I. Bertini and C. Luchinat, "NMR of Paramagnetic Molecules in Biological Systems," The Benjamin/Cummings Publishing Company, Menlo Park (1986), Chap. 7.
54) B. C. Mabbutt and P. E. Wright, *Biochim. Biophys. Acta*, **832**, 175 (1985).